

## Investigation in the Binary System Yb–Ga: Crystal Structure of the Ga-Rich Compound $\text{YbGa}_{3.34}$

Monique Tillard\* and Claude Belin

*Agrégats, Interfaces, Matériaux pour l'Énergie Institut Charles Gerhardt, UMR 5253 CNRS UM2, CC015, Université de Montpellier 2, Sciences et Techniques du Languedoc, 2 Place Eugène Bataillon, 34095 Montpellier Cedex 5, France*

Received June 2, 2009

Compounds within the Yb–Ga binary system were prepared by direct melting of the elements, and their crystal structure was solved from single crystal X-ray diffraction.  $\text{YbGa}_2$  crystallizes in the hexagonal system,  $P6_3/mmc$ ,  $a = 4.4527(2)$ ,  $c = 7.1969(3)$  Å, and  $\text{YbGa}_4$  is monoclinic,  $C2/m$ ,  $a = 6.129(2)$ ,  $b = 6.1096(14)$ ,  $c = 6.097(2)$  Å,  $\beta = 119.05(5)^\circ$ . A new compound of formula  $\text{YbGa}_{3.34}$  was identified in this system, and its crystal structure determined in the orthorhombic  $Immm$  space group,  $a = 4.2049(4)$ ,  $b = 4.3320(5)$ ,  $c = 25.691(3)$  Å. While atoms are fully ordered in  $\text{YbGa}_2$  and  $\text{YbGa}_4$ , partial atomic disorder occurs in  $\text{YbGa}_{3.34}$  where gallium triangular units are found to substitute for some Yb atoms. The electronic structures have been calculated by first principles density functional theory methods using ordered models in supercells. Crystal structures and bonding therein are analyzed on the basis of gallium three-dimensional (3D) anionic networks and are compared with similar compounds.  $\text{YbGa}_{3.34}$  marks the boundary between layered and 3D intergrown gallium frameworks.

### Introduction

Of great interest are compounds formed by the group 13 elements, in which a large variety of inorganic frameworks occur. Combinations with electropositive metal elements lead to fascinating structures characterized by their original anionic sublattices. Gallium in group 13 is located at the Zintl border<sup>1</sup> and, owing to its moderate electronegativity, forms numerous intermetallic phases with alkali metals in which the anionic sublattices are very often built with icosahedral cluster units.<sup>2,3</sup> In these materials that belong to the “Zintl phase” type, bonding within the anionic network may appear mainly covalent; however, the clusters’ electron deficiency requires a description in terms of delocalized bonding.<sup>4–6</sup> Combinations of gallium with alkaline-earth, rare-earth elements, or late transition metals provide other interesting

anionic frameworks. In this rich intermetallic chemistry, gallium shows high flexibility with respect to chemical bonding<sup>7</sup> and tends to mimic carbon in its different forms: diamond, graphite, and fullerene. As an example, gallium is 4-coordinated in  $\text{LiGa}$ <sup>8</sup> with a tetrahedral arrangement and 3-coordinated in  $\text{LaGa}_2$ <sup>9</sup> and  $\text{Li}_{13}\text{Cu}_6\text{Ga}_{21}$ <sup>10</sup> with, respectively, planar hexagonal layer and fullerene-like arrangements.

The recent discovery of  $\text{MgB}_2$  superconductivity, with a critical temperature of 39 K,<sup>11</sup> has generated a great deal of excitement because this compound displays the widely spread  $\text{AlB}_2$  structural type, and it is a common commercial compound. Subsequently, a lot of research has been focused on atomically substituted  $\text{MgB}_2$  derivatives to improve the superconducting properties. Some gallium alloys, for example,  $\text{V}_3\text{Ga}$  and  $\text{Nb}_3\text{Ga}$ , have been known for a long time as being superconducting below 10–15 K,<sup>12</sup> and more recently  $\text{PuCoGa}_5$  was reported with a transition around 22 K.<sup>13,14</sup> With the prospect of discovering new gallides presenting

\*To whom correspondence should be addressed. E-mail: mtillard@univ-montp2.fr. Phone: 33 4 67 14 48 97. Fax: 33 4 67 14 33 04.

(1) Schafer, H.; Eisenmann, B.; Muller, W. *Angew. Chem., Int. Ed. Engl.* **1973**, *12*, 694–712.

(2) Belin, C.; Tillard-Charbonnel, M. *Prog. Solid State Chem.* **1993**, *22*, 59–109.

(3) Belin, C.; Tillard-Charbonnel, M. *Coord. Chem. Rev.* **1998**, *180*, 529–564.

(4) Wade, K. *Adv. Inorg. Chem. Radiochem.* **1976**, *18*, 1–66.

(5) Mingos, D. P.; Wales, D. *Introduction to cluster chemistry*; Prentice Hall: Englewood Cliffs, NJ, 1990.

(6) Tillard-Charbonnel, M.; Manteghetti, A.; Belin, C. *Inorg. Chem.* **2000**, *39*, 1684–1696.

(7) Haarmann, F.; Koch, K.; Gruner, D.; Schnelle, W.; Pecher, O.; Cardoso-Gil, R.; Borrmann, H.; Rosner, H.; Grin, Y. *Chem.—Eur. J.* **2009**, *15*, 1673–1675.

(8) Zintl, E.; Brauer, G. *Z. Phys. Chem.* **1933**, *B20*, 245–271.

(9) Zheng, C.; Mattausch, H.; Simon, A. *Z. Kristallogr.* **2001**, *216*, 497.

(10) Tillard-Charbonnel, M.; Belin, C. *J. Solid State Chem.* **1991**, *90*, 270–278.

(11) Nagamatsu, J.; et al. *Nature* **2001**, *410*, 63.

(12) Testardi, L. R.; Soden, R. R.; Greiner, E. S.; Wernick, J. H.; Chirba, V. G. *Phys. Rev.* **1967**, *154*, 399–401.

(13) Sarrao, J. L.; Morales, L. A.; Thompson, J. D.; Scott, B. L.; Stewart, G. R.; Wastin, F.; Rebizant, J.; Boulet, P.; Colineau, E.; Lander, G. H. *Nature* **2002**, *420*, 297–299.

(14) Griveau, J. C.; Pfeleiderer, C.; Boulet, P.; Rebizant, J.; Wastin, F. *J. Magn. Magn. Mater.* **2004**, *272–276*, 154–155.

similar features, we have investigated some gallium alloys involving rare-earth and transition elements. The studies on the Sm–Co–Ga system were motivated by the chemical analogies between Sm and Pu. A new compound,  $\text{Sm}_4\text{Co}_3\text{-Ga}_{16}$ , which is a superstructural derivative of  $\text{SmCoGa}_5$ , was found to be superconducting with  $T_c \sim 2.8$  K.<sup>15</sup> Meanwhile, some attention has also been paid to the Sm–Ga binary phase structures and especially to  $\text{SmGa}_{2.67}$  which displays an unusual gallium anionic framework mixing planar hexagonal layers and opened polyhedral units.<sup>16</sup> This so-called  $\epsilon$  phase, with a fairly wide composition domain in the Sm–Ga binary, is also expected in the binary system containing Yb. A revised version of the Yb–Ga binary phase diagram published in 1992 reports five line compounds:  $\text{Yb}_2\text{Ga}$ ,  $\text{YbGa}$ ,  $\text{YbGa}_2$ ,  $\text{YbGa}_4$ , and  $\text{YbGa}_6$  characterized from X-ray powder data.<sup>17</sup> In addition,  $\text{YbGa}_{3-x}$  is claimed to exist within a narrow solubility range (25 to 27.4 at. % Yb) and  $\text{Yb}_3\text{Ga}_8$  only above 830 °C.<sup>18</sup>  $\text{YbGa}_4$  was first reported in the tetragonal  $\text{BaAl}_4$ -type on the basis of its X-ray powder pattern<sup>19</sup> and, later on, in the monoclinic  $\text{CaGa}_4$ -type.<sup>20</sup> During a study of pressure induced changes in the  $\text{YbGa}_2$  structural and electronic properties, it has been shown that  $\text{YbGa}_2$  undergoes a phase transition from  $\text{CaIn}_2$  to  $\text{UHg}_2$  type and the Yb atoms realize the +2 oxidation state at ambient pressure.<sup>21</sup> More recently, the Ga-rich compound  $\text{YbGa}_5$  was identified, and the phase diagram redetermined in the composition range from Ga to  $\text{YbGa}_4$ . The tetragonal single crystal structure of  $\text{YbGa}_5$  was described in both ordered and disordered variants.<sup>22</sup>

This paper reports the synthesis and single crystal structure determination of the new gallium-rich intermetallic compound  $\text{YbGa}_{3.34}$ . The structures of  $\text{YbGa}_2$  and  $\text{YbGa}_4$ , thoroughly determined from single crystal data, are compared to previous results.

## Experimental Section

Our aim was to synthesize phases in the stoichiometry range 20–32 at. % Yb close to compounds  $\text{YbGa}_{3-x}$  and  $\text{Yb}_3\text{Ga}_8$ . An alloy was prepared from the elements taken in the (1:3) proportion. The elements were inserted into a tantalum tube, which was sealed under argon atmosphere at both ends by arc welding. The Ta container was protected from oxidation inside an evacuated silica jacket, heated up to 850 °C for 24 h for reaction, annealed at 720 °C for 72 h and finally cooled down to room temperature at the rate of 10°/h. As the product appeared fairly well crystallized, several small metal-like shiny crystals were chosen under a microscope in a glovebox, mounted inside Lindemann capillaries, and tested for singularity on a CCD Xcalibur four-circle diffractometer (Oxford Diffraction) operating with monochromated  $\text{Mo K}\alpha$  radiation. The best diffracting crystal was selected for data collection on the CCD diffractometer at room temperature over the angular  $2\theta$  domain ranging from 6 to 69°. The reflection intensities were extracted from 1246 frames

recorded with standard exposure times of 23 s at a crystal-detector distance of 50 mm. The cell parameters were determined and refined with all the integrated peaks using the Xcalibur CrysAlis software.<sup>23</sup> The main crystallographic details and the experimental parameters are given in Table 1.

The set of 15975 reflections (including symmetry equivalent and redundant ones) recorded over the complete diffraction sphere was indexed in an orthorhombic I-centered cell of parameters  $a = 4.2049(4)$ ,  $b = 4.3320(5)$ ,  $c = 25.691(3)$  Å. The reflections were corrected for absorption effects using the SCALE3ABS numerical procedure included in the CrysAlis RED software. The data set used for final refinement in the *Immm* orthorhombic space group consisted of 611 independent reflections among which 582 were observed according to the criterion  $I > 2\sigma(I)$ . The structure was solved by direct methods with the program SHELXS97.<sup>24</sup> Two Yb and four Ga positions were assigned and refined isotropically using SHELXL97<sup>25</sup> to a reliability factor of  $\sim 17\%$ . Free refinement of occupation factors suggested an incomplete filling of the Yb2 site. On the other hand, two high intensity peaks remaining in the subsequent Fourier difference were found abnormally close to this position. They were assigned to gallium atoms and consequently refined with partial occupancies, as for Yb2. Within the standard deviation limits, gallium site occupations freely converged to values that compensate for the deficiency of Yb2 atom. Actually, in this disordered configuration, Yb2 is partially replaced at site 2a by a gallium triangle formed of one Ga5 and two Ga6 atoms. In the next steps, site occupancies were refined using appropriate linear constraints and anisotropic atomic displacement parameters were applied to all atoms. The refined composition is  $\text{Yb}_{0.89}\text{Ga}_{2.97}$  ( $\text{YbGa}_{3.34}$ ), which is in good agreement with the semiquantitative EDX analyses (Yb/Ga = 0.30) of several single crystals formerly characterized by X-ray diffraction.

Thermal ellipsoids of atoms Ga1 and Ga3 belonging to the hexagonal cycle are quite elongated along the  $a$ -axis. Short interatomic distances of 2.327(7) and 2.357(6) Å are observed between hexagons and the inner triangle. They cannot be corrected for correlated atomic thermal motions because they result from the local atomic disorder created by the statistical replacement of Yb2. After removing Ga1 and Ga3 atoms, a precise Fourier difference synthesis clearly indicated satellites in the electron density on both sides of plane (100). Refinements were then carried out using complementary occupancies for Ga1\* at 0.396, 0, 0.0957 and Ga1 at 1/2, 0, 0.0958 as well as for Ga3\* at 0.394, 1/2, 0.0496 and Ga3 at 1/2, 1/2, 0.0482 (Ga1\* and Ga3\* stand for Yb2 replacement). Anisotropic refinement of only Ga1 and Ga3 led to a final reliability factor  $R1$  of 5.42%. Isotropic refinement with split positions slightly increased the  $R1$  factor to 5.71% but yielded larger triangle-to-hexagon distances of 2.75(1) and 2.74(1) Å. They are to be compared with the Ga–Ga distances of 2.70 Å found in  $\text{YbGa}_{2.64}$  for similar coordinations.<sup>18</sup> Although this acute disorder problem might suggest an undetected larger cell, reflection data sets recorded for several single crystals do not contain any additional diffraction spots regardless of the exposure time. Furthermore, attempts to solve and refine the structure in lower symmetries down to the triclinic *P1* space group always indicated the occurrence of gallium triangular units substituting for Yb2 atoms.

The congruently melting compound  $\text{YbGa}_2$  was prepared from a stoichiometric mixture of the elements heated to 1100 °C

(15) Jia, Y. Z.; Belin, C.; Tillard, M.; Lacroix-Orio, L.; Zitoun, D.; Feng, G. H. *Inorg. Chem.* **2007**, *46*, 4177–4186.

(16) Tillard, M.; Zitoun, D.; Belin, C. *Inorg. Chem.* **2009**, *48*, 2399–2406.

(17) Palenzona, A.; Cirafici, S. *J. Phase Equilib.* **1992**, *13*, 32–35.

(18) Cirafici, S.; Fornasini, M. L. *J. Less-Common Met.* **1990**, *163*, 331–338.

(19) Krypuyakevych, P. I.; Gladyshevskii, E. I.; Dzyana, D. I. *Kristallografiya* **1965**, *10*, 471.

(20) Palenzona, A.; Cirafici, S. *J. Less-Common Met.* **1979**, *63*, 105–109.

(21) Schwarz, U.; Giedigkeit, R.; Niewa, R.; Schmidt, M.; Schnelle, W.; Cardoso, R.; Hanfland, M.; Hu, Z.; Klementiev, K.; Grin, Y. Z. *Anorg. Allg. Chem.* **2001**, *627*, 2249–2256.

(22) Giedigkeit, R.; Niewa, R.; Schnelle, W.; Grin, Y.; Kniep, R. *Z. Anorg. Allg. Chem.* **2002**, *628*, 1692–1696.

(23) CrysAlis'Red' 171 software package; Oxford Diffraction Ltd.: Abingdon, U.K.

(24) Sheldrick, G. M. *SHELXS 97, A Program for Crystal Structures Solution*; University of Göttingen: Göttingen, Germany, 1997.

(25) Sheldrick, G. M. *SHELXL97, A Program for Refining Crystal Structures*; University of Göttingen: Göttingen, Germany, 1997.

Table 1. Crystallographic Details and Experimental Parameters

crystal system	orthorhombic	hexagonal	monoclinic
space group, number	<i>Immm</i> , 71	<i>P6<sub>3</sub>/mmc</i> , 194	<i>C2/m</i> , 12
unit cell parameters			
<i>a</i> , Å	4.2049(4)	4.4527(2)	6.129(2)
<i>b</i> , Å	4.3320(5)		6.109(1)
<i>c</i> , Å	25.691(3)	7.1969(3)	6.097(2)
$\beta$ , deg			119.05(5)
volume (Å <sup>3</sup> )	467.98(9)	123.573(9)	199.58(10)
formula	Yb <sub>0.89</sub> Ga <sub>2.97</sub> ("YbGa <sub>3.34</sub> ")	YbGa <sub>2</sub>	YbGa <sub>4</sub>
<i>Z</i>	6	2	2
formula weight	360.96	312.48	451.92
density	7.685	8.398	7.520
absorption coeff. (mm <sup>-1</sup> )	51.48	58.75	49.60
extinction coeff. ( $\times 10^{-4}$ )	8(1)	24(6)	36(9)
<i>F</i> (000)	925	264	388
crystal size (mm)	0.22 $\times$ 0.14 $\times$ 0.05	0.10 $\times$ 0.09 $\times$ 0.09	0.18 $\times$ 0.15 $\times$ 0.07
refinement method	full matrix least-squares on <i>F</i> <sup>2</sup>	full matrix least-squares on <i>F</i> <sup>2</sup>	full matrix least-squares on <i>F</i> <sup>2</sup>
reflins collected	15975	3106	2678
$\theta$ range (deg)	3.17–34.50	5.29–34.47	3.82–34.14
independent reflins	611 [ <i>R</i> <sub>int</sub> = 0.084]	123 [ <i>R</i> <sub>int</sub> = 0.050]	445 [ <i>R</i> <sub>int</sub> = 0.063]
observed reflins/refined params	582/37	111/7	431/17
GOF on <i>F</i> <sup>2</sup>	1.27 ( <b>1.23</b> ) <sup>a</sup>	1.34	1.28
final indices <i>R</i> 1 <sup>b</sup> [ <i>I</i> > 2 $\sigma$ ( <i>I</i> )]	0.0542 ( <b>0.0571</b> ) <sup>a</sup>	0.0126	0.0590
w <i>R</i> 2 <sup>a</sup> [ <i>I</i> > 2 $\sigma$ ( <i>I</i> )]	0.1249 ( <b>0.1290</b> ) <sup>a</sup>	0.0281	0.1247
<i>R</i> 1 (all data)	0.0566 ( <b>0.0597</b> ) <sup>a</sup>	0.0224	0.0609
w <i>R</i> 2 (all data)	0.1259 ( <b>0.1224</b> ) <sup>a</sup>	0.0293	0.1255
largest diff. peak and hole (e Å <sup>-3</sup> )	3.79/−3.07 ( $\pm$ 3.9) <sup>a</sup>	1.38/−1.42	3.95/−5.15

<sup>a</sup> Italic bold values corresponds to agreement factors for refinement of Ga1 and Ga3 in split positions. <sup>b</sup>  $R1 = \sum ||F_o| - |F_c|| / \sum |F_o|$ , w*R*2 =  $[\sum w(F_o^2 - F_c^2)^2 / \sum w(F_o^2)]^{1/2}$ .

for 2 h then cooled at 10°/h to 850 °C, annealed for 48 h at this temperature, and finally cooled down to room temperature (50°/h). The structure was solved and refined in the hexagonal space group *P6<sub>3</sub>/mmc* using a set of 123 independent reflections.

To prepare YbGa<sub>4</sub>, a mixture of elements at 19.6 at. % Yb was heated up to 900 °C, kept for 15 h for homogenization, and cooled to 600 °C at 10°/h and then to room temperature at 20°/h. As shown in the available diagrams,<sup>17,22</sup> phase equilibria are very intricate in this concentration range. A slow cooling of the sample leads, below 830 °C, to the crystallization first of YbGa<sub>2</sub> and thereafter of YbGa<sub>4</sub>. Relying on the phase diagram, crystallization would begin at liquidus, below 830 °C, and the formation of Yb<sub>3</sub>Ga<sub>8</sub> should not be observed since this compound is reported to be stable only between 830 and 870 °C.<sup>18</sup> The heterogeneous resulting product contains a large amount of YbGa<sub>4</sub> crystals (YbGa<sub>4</sub> to YbGa<sub>2</sub> ratio is about 4.5 according to the level rule). It should be noted that, according to the differential thermal analyses (DTA) experiments carried out in this work, the product of the reaction would contain also a small amount of the compound YbGa<sub>3.34</sub>. YbGa<sub>4</sub> single crystals were selected under microscope and tested on the CCD diffractometer. The structure was solved and refined in the *C2/m* monoclinic space group using a set of 445 independent reflections.

As it can be seen in Table 1, resolution of the single crystal structure of YbGa<sub>2</sub> is more accurate than those of YbGa<sub>4</sub> and YbGa<sub>3.34</sub> of which the final electron residual values are larger (3.95 at  $\sim$ 1 Å from Yb and 3.79 at  $\sim$ 0.5 Å from Ga5, respectively); this is due to the difficulty in obtaining excellent quality single crystal data for these non-congruently melting or peritectally decomposing compounds.

DTA were performed with a Setaram Labsys analyzer for a sample of YbGa<sub>3.34</sub> prepared as described above and for two samples having quite close compositions. Either the crystalline pieces selected from the YbGa<sub>3.34</sub> preparation or the mixture of elements in desired amounts were inserted in niobium crucibles then sealed under argon atmosphere. Calibration accuracy was verified by measuring the fusion

temperature of pure elements (Al, Ag) indicating a maximal standard deviation of 2 °C. For the YbGa<sub>3.34</sub> sample (23.04 at. % Yb), two endothermic events are observed at 756 °C (small amplitude) and at 764 °C (large amplitude) on the heating curve. They correspond to the peritectic decompositions of a small amount of YbGa<sub>4</sub> (present as a side product) and of the YbGa<sub>3.34</sub> compound, respectively. The end of melting (liquidus curve) is observed at 946 °C. These two endothermic events are also found for the sample at 22.7 at. % Yb. Instead, the heating curve of sample at 24.9 at. % Yb displays two endothermic events at 748 and 764 °C, the latter corresponds to the peritectic decomposition of YbGa<sub>3.34</sub> while the former would correspond to the peritectic invariant associated to the YbGa<sub>3-x</sub> compound and reported at  $\sim$ 740 °C.<sup>17</sup> No thermal event could be detected in the temperature domain between 830 and 870 °C, and this could raise the question of the existence of compound Yb<sub>3</sub>Ga<sub>8</sub>. It should be noticed that, in the light of recent single crystal studies, the stoichiometries of compounds M<sub>3</sub>Ga<sub>8</sub> (M = Eu, Sr) have been revised into M<sub>3-x</sub>Ga<sub>8+3x</sub>. Thus we can wonder whether the Yb<sub>3</sub>Ga<sub>8</sub> compound,<sup>18</sup> whose formulation was based on the comparison with Eu<sub>3</sub>Ga<sub>8</sub>, is not actually YbGa<sub>3.34</sub>. However, obtaining the formal evidence would require additional detailed thermal investigations in the range of composition delimited by YbGa<sub>4</sub> and YbGa<sub>2</sub>.

### Calculation Methods

Calculations were performed at the density functional theory (DFT) level with VASP and CASTEP codes using the gradient-corrected GGA-PBE exchange and correlation functional.<sup>26</sup> Accurate geometry optimizations were carried out with VASP<sup>27–29</sup> that uses a plane-wave basis set and the

(26) Perdew, J. P.; Burke, K.; Ernzerhof, M. *Phys. Rev. Lett.* **1996**, *77*, 3865.

(27) MedeA-VASP, is a commercial package that provides a graphical interface to set up, run, and analyze VASP calculations under Windows environment; Materials Design Inc.

(28) Kresse, G.; Furthmüller, J. *Phys. Rev. B* **1996**, *54*, 11169.

(29) Kresse, G.; Furthmüller, J. *J. Comput. Mater. Sci.* **1996**, *6*, 15.

**Table 2.** Positional and Atomic Displacement Parameters for Atoms in YbGa<sub>3.34</sub>

atom	site	x	y	z	occupation	$U_{eq}$
Ga1	4j	0.5	0	0.09576(10)	1	0.0399(9)
Ga2	4i	0	0	0.25137(9)	1	0.0169(4)
Ga3	4i	0.5	0.5	0.04862(10)	1	0.0402(9)
Ga4	4j	0.5	0	0.19145(9)	1	0.0184(5)
Ga5	4i	0	0	0.0543(5)	0.151(7)	0.019(4)
Ga6	8l	0	0.297(5)	0.0304(7)	0.151(7)	0.044(5)
Yb1	4j	0.5	0	0.35090(4)	1	0.0188(3)
Yb2	2a	0	0	0	0.670(7)	0.0180(5)

projector augmented wave technique (PAW) which aims to achieve simultaneously the computational efficiency of the pseudo potential method and the accuracy of the full potential linearized augmented plane wave (FLAPW) method. CASTEP<sup>30</sup> uses plane-wave basis sets to treat valence electrons and pseudo potentials to approximate the potential field of ion cores. Ultrasoft pseudo potentials (USPP) generated for each element according to the Vanderbilt<sup>31</sup> scheme were used. Since Yb 5s and 5p high-lying shallow-core may hybridize with 5d and 4f orbitals, ultrasoft pseudo potentials treat them as valence states. The inner 3d levels of Ga were also considered as valence states. Kinetic cutoff energies were set at fine qualities. Monkhorst–Pack uniform grids<sup>32</sup> of automatically generated k-points were used.

### Structural Description

The structure of the new compound YbGa<sub>3.34</sub> was solved and refined in the orthorhombic *Immm* space group. Atomic positions and equivalent displacement parameters are given in Table 2. Gallium atoms form a three-dimensional (3D) framework built of rhombic diamond-faceted layers perpendicular to the *c*-axis associated with planar hexagon-based ribbons stacked along the *a*-axis (Figure 1). Yb1 atoms are located at site 4j (1/2 0 *z*) between these different units. The Yb2 atoms at site 2a (0 0 0) are positioned between ribbons, capping the Ga hexagons. Atomic disorder occurs at site 2a, only filled by Yb2 at 67%. Triangular gallium units composed of Ga5 and Ga6 atoms respectively sitting at sites 4i and 8l are found to complement Yb2 atoms. The structure is close to that reported for compound Yb<sub>3</sub>Ga<sub>8</sub>.<sup>18</sup> However, in the latter, all the ytterbium positions are fully occupied without occurrence of disorder (Figure 2). Compounds YbGa<sub>3.34</sub> and Yb<sub>3</sub>Ga<sub>8</sub> display very similar cell parameters, and their structures are to be compared with the tetragonal structure of YbGa<sub>5</sub>.<sup>22</sup> In Yb<sub>3</sub>Ga<sub>8</sub>, all the Yb atoms fully occupy their sites while they are partially replaced by triangular Ga<sub>3</sub> units in YbGa<sub>3.34</sub> or by Ga<sub>2</sub> dumbbells in YbGa<sub>5</sub> (Figure 2). These three structures may be considered as deriving from that of YbGa<sub>4</sub> (Figure 3) by the cross intergrowth of rhombic corrugated layers and hexagon-based ribbons of gallium (Figure 2). The main difference between the three structures stems from the capping of hexagons: Yb atom in Yb<sub>3</sub>Ga<sub>8</sub>, Ga<sub>2</sub> dumbbell in YbGa<sub>5</sub>, and Ga<sub>3</sub> triangle in YbGa<sub>3.34</sub>.

Such substitution of cations by gallium triangular units has been already observed, to a lesser extent, in other orthorhombic gallide structures derived from the M<sub>3</sub>Ga<sub>8</sub> structural model. In Sr<sub>3-x</sub>Ga<sub>8+3x</sub>, some disorder occurs at one cation position through the partial replacement of Sr (15%) by

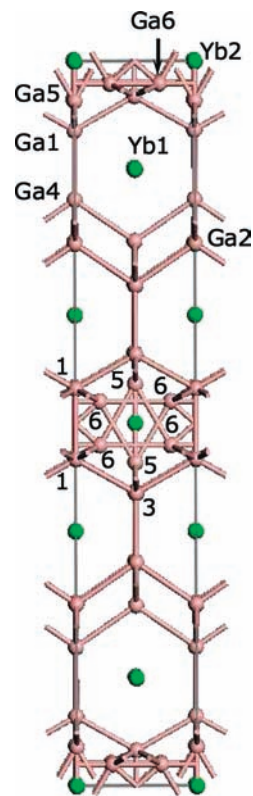


**Figure 1.** Representation of the crystal structure of YbGa<sub>3.34</sub>, orthorhombic, *Immm*,  $a = 4.2049(4)$ ,  $b = 4.3320(5)$ ,  $c = 25.691(3)$  Å, projected along the [100] direction. Atomic disorder occurs at (0 0 0) and (1/2 1/2 1/2) where gallium triangles partially substitute for Yb2 atoms.

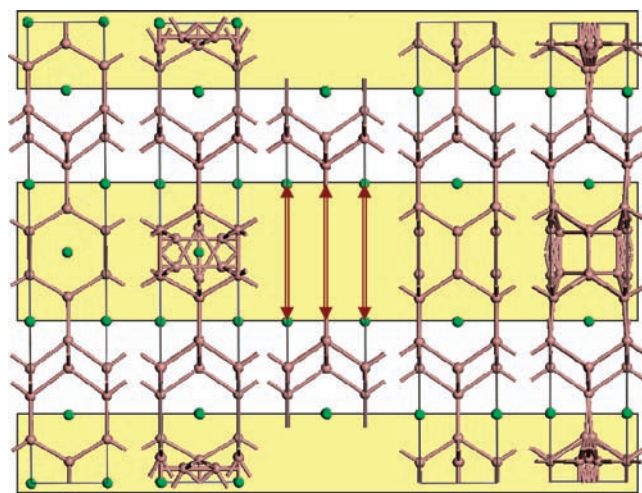


**Figure 2.** Structures of Yb<sub>3</sub>Ga<sub>8</sub>, YbGa<sub>3.34</sub>, YbGa<sub>4</sub>, and the ordered and disordered variants of YbGa<sub>5</sub> (left to right), based on the packing of interlinked rhombic layers (white domain) directly connected in YbGa<sub>4</sub>. Between these rhombic layers, may intercalate hexagonal sublattices (yellow domain) that differ by the hexagon capping: Yb atom in Yb<sub>3</sub>Ga<sub>8</sub>, Ga<sub>3</sub> triangle in YbGa<sub>3.34</sub>, and Ga<sub>2</sub> dumbbell in YbGa<sub>5</sub>.

triangular gallium units.<sup>33</sup> The same type of disorder is found in Eu<sub>3-x</sub>Ga<sub>8+3x</sub> with a 12% replacement of one Eu atom in addition to a slight out of plane shift of the gallium atoms forming the hexagon.<sup>34</sup> Using the same argumentation for

(30) Payne, M. C.; Teter, M. P.; Allan, D. C.; Arias, T. A.; J.D., J. *Rev. Mod. Phys.* **1992**, *64*, 1045.

(31) Vanderbilt, D. *Phys. Rev. B* **1990**, *41*, 7892–7895.

(32) Monkhorst, H. J.; Pack, J. D. *Phys. Rev. B* **1997**, *16*, 1748.

(33) Haarmann, F.; Prots, Y.; Gobel, S.; Von Schnering, H. G. Z. *Kristallogr.* **2006**, *221*, 257–258.

(34) Sichevich, O. M.; Prots, Y.; Grin, Y. Z. *Kristallogr.* **2006**, *221*, 265–266.

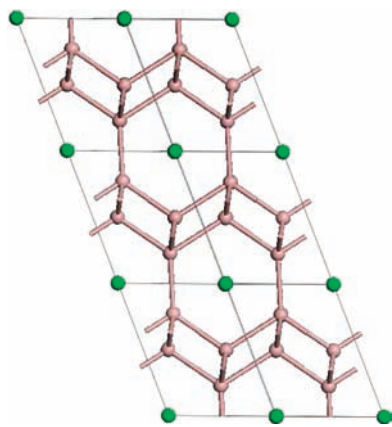


**Figure 3.** Projection of the  $\text{YbGa}_4$  structure, monoclinic,  $C2/m$ ,  $a = 6.129(2)$ ,  $b = 6.1096(14)$ ,  $c = 6.097(2)$  Å,  $\beta = 119.05(5)^\circ$  onto the (101) plane. The rhombic gallium layers are interconnected through Ga–Ga bonds of 2.464(4) Å.

$\text{Yb}_3\text{Ga}_8$ , substitution at one cationic site of 33% of Yb atoms would lead to  $\text{YbGa}_{3.34}$  which might be formally described as  $\text{Yb}_{3-x}\text{Ga}_{8+3x}$  with  $x = 0.32$ . This interpretation would imply the existence of a composition domain ranging, at least, from 23.0 to 27.3 at % Yb ( $0 \leq x \leq 0.32$ ) and the survival of  $\text{Yb}_3\text{Ga}_8$  structure below 830 °C.

No intergrowth was found in the 3D network of  $\text{YbGa}_4$  where corrugated rhombic gallium layers (Ga–Ga bonds of 2.574(2) and 2.625(3) Å) are directly connected to alike units through quite short Ga–Ga bonds of 2.464(4) Å. As it was previously reported, the indexation of the X-ray powder pattern of  $\text{YbGa}_4$  according to the tetragonal  $\text{BaAl}_4$ -type structure leaves unassigned lines, suggesting a different structure for this compound.<sup>20</sup> The analysis of Cirafici and Fornasini<sup>18</sup> based on powder XRD data later confirmed that  $\text{YbGa}_4$  is isotopic with  $\text{CaGa}_4$ , the structure of which is being already described as a monoclinic distortion of  $\text{BaAl}_4$ .<sup>35</sup> The  $C2/m$  monoclinic structure of  $\text{YbGa}_4$  is confirmed by our single crystal structure determination.

The structure of  $\text{YbGa}_2$  determined from single crystal data is hexagonal,  $P6_3/mmc$ , and confirms the previous results from X-ray diffraction.<sup>36,21</sup> The atomic arrangement (Figure 4) consists of corrugated hexagonal layers of gallium that are interconnected along  $c$ -axis, the Yb atoms sitting in the interlayer channels. This structure is of the  $\text{CaIn}_2$ -type and is different from those of most  $\text{LnGa}_2$  lanthanide gallium compounds that crystallize in the  $\text{AlB}_2$ -type ( $P6/mmm$ ) with gallium planar hexagonal layers and with a periodicity reduced by half along  $c$ -axis.

### Electronic Structures and Discussion

DFT calculations were carried out for the compounds  $\text{YbGa}_2$ ,  $\text{YbGa}_{3.34}$ , and  $\text{YbGa}_4$  to complement our structural determinations and to answer questions arising when considering the formation, bonding and structural stability of each compound.

Let us first examine  $\text{YbGa}_2$  which has the smaller unit cell ( $Z = 2$ ). Geometry optimizations were performed using the code VASP starting both from the experimental  $P6_3/mmc$  structure ( $a = 4.45$ ,  $c = 7.19$  Å) and from a hypothetical  $P6/mmm$  model

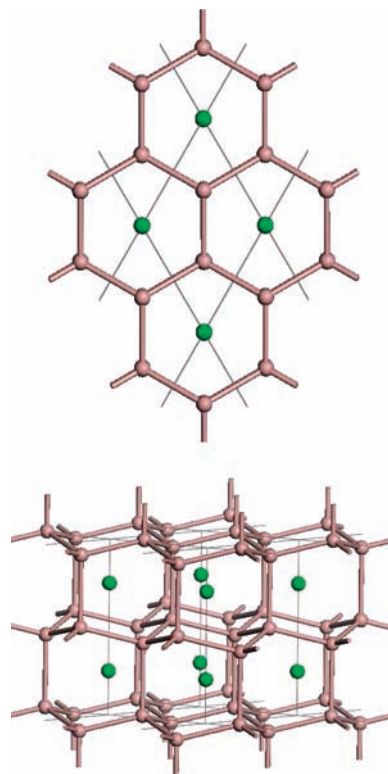


**Figure 4.**  $\text{YbGa}_2$  structure, hexagonal,  $P6_3/mmc$  with  $a = 4.4527(2)$ ,  $c = 7.1969(3)$  Å: up, projected along [001]; down, nearly viewed along [110]. The corrugated hexagonal layers of gallium are interconnected along  $c$ -axis through Ga–Ga bonds of 3.007(2) Å.

( $a = 4.45$ ,  $c = 8.20$  Å). The latter has been built with two planar hexagonal layers of gallium stacked along  $c$ -axis like in  $\text{LaGa}_2$  ( $P6/mmm$ ,  $\text{AlB}_2$ -type) after doubling the unit cell along  $c$ -axis. Prior to optimization, atoms were slightly moved aside their crystallographic original Wyckoff positions to avoid convergence into false energy minima, then atomic coordinates and cell parameters were allowed to vary in  $P1$  symmetry.

Under these conditions, the symmetry  $P6_3/mmc$  is retained when starting from the experimental model with cell parameter deviations less than 0.5%. The  $P6/mmm$  hypothetical model undergoes drastic modifications toward the  $P6_3/mmc$  symmetry: cell contraction of about 12% along the  $c$ -axis, waving and interconnection of gallium layers. For  $\text{YbGa}_2$ , this undoubtedly marks the neat preference for a structural model in which the Ga hexagonal layers are close enough (3.007(2) Å) to be involved, through a 3-bonded to 4-bonded Ga atoms reorganization, in bonding interactions as visualized in the CASTEP electron density difference map (Figure 5). This is in agreement with the topological analyses of the electron localization function in  $\text{CaGa}_2$ <sup>7</sup> and in  $\text{YbGa}_2$ <sup>21</sup> showing that this long contact between the waved gallium layers is a bonding contact.

A very complete study of digallides of Ca, Sr, and Ba, mainly based on NMR measurements and electronic structure calculations has shown that in the series the structure changes from the  $\text{CaIn}_2$ -type for  $\text{CaGa}_2$  to the  $\text{AlB}_2$ -type for  $\text{SrGa}_2$  and  $\text{BaGa}_2$ .<sup>7</sup> Waved hexagonal layers also exist in  $\text{MgGa}_2$ ,<sup>37</sup>  $\text{ScGa}_2$ ,<sup>38</sup> and in the high-pressure form of

(37) Ellner, M.; Gödecke, T.; Duddek, G.; Predel, B. Z. *Anorg. Allg. Chem.* **1980**, *463*, 170–178.

(38) Belyavina, N. N.; Markiv, V. Y. *Dopov. Akad. Nauk Ukr. RSR (Ser. A)* **1980**, *4*, 87.

(35) Bruzzone, G.; Fornasini, M. L.; Merlo, F. *J. Less-Common Met.* **1989**, *154*, 67–77.

(36) Iandelli, A. *J. Less-Common Met.* **1987**, *135*, 195–198.

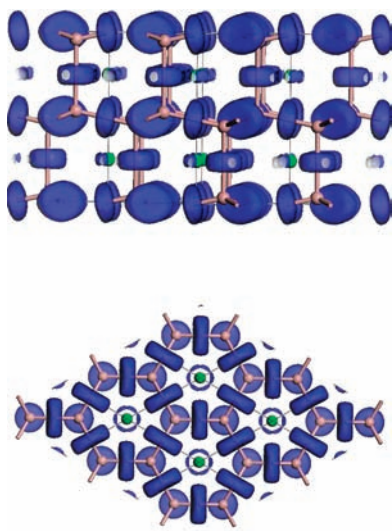


**Figure 5.** Two views of the 3D electron density difference calculated with program CASTEP, isovalue level of  $0.025 \text{ e } \text{\AA}^3$ , emphasizing the interlayer (up) and the intralayer (down) bonding.

$\text{GdGa}_2$ .<sup>39</sup> With short cation-to-gallium distances of 2.87 and 2.98 Å, the Mg and Ca compounds display the  $P6_3/mmc$  symmetry while with larger distances of 3.45 and 3.60 Å,  $\text{SrGa}_2$  and  $\text{BaGa}_2$  compounds crystallize in  $P6/mmm$ . In  $\text{ScGa}_2$  ( $\text{Sc}-\text{Ga} = 2.94 \text{ \AA}$ ), the waved gallium layers and their interconnections are, owing to symmetry  $Imma$  ( $\text{KHg}_2$ -type), somewhat different from those in the  $P6_3/mmc$  ( $\text{CaIn}_2$ -type) structure. In Y and La digallides, with cation-to-gallium distances of, respectively, 3.18 and 3.32 Å, the gallium network adopts the planar hexagonal geometry.<sup>40,9</sup>

It is well-known that the ionic radii of lanthanide elements decrease along the series because of the poor shielding of nuclear charge by 4f electrons, this contraction explaining the smallest radius of ytterbium. In intermetallic compounds, Yb is very seldom trivalent, and its normal state is divalent as shown in  $\text{YbGa}_2$  from XANES experiments.<sup>21</sup> So, it compares better with calcium and magnesium, rather than with trivalent rare earths. The Yb–Ga distance is rather short (2.9783(4) Å) in  $\text{YbGa}_2$  compared to other lanthanide digallides. Hence,  $\text{YbGa}_2$  adopts the  $P6_3/mmc$  structure that is preferred by  $\text{MGa}_2$  compounds containing small and divalent cations.

With a higher content in gallium,  $\text{YbGa}_4$  crystallizes in the monoclinic  $\text{CaGa}_4$ -type while most of  $\text{MGa}_4$  compounds display the tetragonal  $\text{BaAl}_4$ -type structure that had been referred to as the “most populous structural type”.<sup>41</sup> Actually,  $\text{BaAl}_4$ -type is adaptable to different electron concentrations because the 16-vertex cavity (corner-truncated tetragonal prism) can accommodate any kind of cation.<sup>42</sup> Except  $\text{CaGa}_4$ , the tetragallides  $\text{MGa}_4$  ( $\text{M} = \text{Na}, \text{Ba}, \text{Eu}, \text{Sr},$  and  $\text{Yb}$ ) listed in the Pearson database are assigned the tetragonal  $\text{BaAl}_4$ -type ( $I4/mmm$ ). Note that only two lanthanide tetragallides are known:  $\text{EuGa}_4$ <sup>43</sup> which belongs to

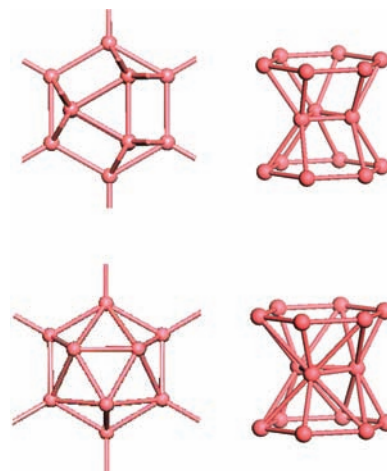


**Figure 6.**  $\text{Ga}_{15}$  units (projection and front view) resulting from fusion by triangle sharing of two hemicuboctahedra (up) and of two hemi-icosahedra (down).

$\text{BaAl}_4$ -type and  $\text{YbGa}_4$  which was first described in 1965<sup>19</sup> as isotopic with tetragonal  $\text{CaGa}_4$ . In a subsequent work, authors pointed out that for  $\text{YbGa}_4$  some reflections could not be accounted for with this structure.<sup>20</sup> Ever since a single crystal structure determination definitely proved  $\text{CaGa}_4$  to really be monoclinic  $C2/m$ ,<sup>35</sup> an alternate description was then proposed for  $\text{YbGa}_4$ ,<sup>18</sup> relying on the similarity of their powder patterns. Our present single crystal X-ray analysis unambiguously validates the  $C2/m$  symmetry for  $\text{YbGa}_4$ .

VASP and CASTEP geometry optimizations were carried out to check the stability of  $\text{YbGa}_4$  in its monoclinic form using the same procedure as described above for  $\text{YbGa}_2$ . We started from the experimental  $C2/m$  structure and from the dubious tetragonal  $I4/mmm$  model. To save computational time, calculations were done using the primitive cells. The refined experimental structure still displays the  $C2/m$  symmetry with cell parameters variations less than 1.4%. On the other hand, starting from the tetragonal model with parameters taken from ref 20, the refined atom positions perfectly matched the  $C2/m$  monoclinic symmetry as detected, at the lowest tolerance level of  $10^{-3} \text{ \AA}$ , by the “Find symmetry” tool provided by Materials Studio.<sup>30</sup> The loss of tetragonal symmetry is highlighted by atomic displacements of nearly 0.03 Å from the initial positions, which means the distortion from tetragonal  $I4/mmm$  into monoclinic  $C2/m$  remains rather weak.

The structure of  $\text{YbGa}_{3,34}$ , orthorhombic  $Immm$ , is much more complex. In addition to rhombic layers packed along the  $c$ -axis, the 3D network of gallium contains hexagon-based ribbons stacked in the perpendicular direction, along the  $a$ -axis. According to the local disorder around site 2a, the gallium triangles that substitute for one-third of Yb atoms lie between two Ga hexagons. The resulting  $\text{Ga}_{15}$  units have already been observed in disordered structures of  $\text{YbGa}_{2,64}$ <sup>18</sup> and  $\text{SmGa}_{2,67}$ <sup>16</sup> where they display different morphologies. They result from the fusion, by triangle-sharing, of two hemicuboctahedra in  $\text{SmGa}_{2,67}$  and of two hemi-icosahedra in  $\text{YbGa}_{2,64}$  and  $\text{YbGa}_{3,34}$  (Figure 6). Both  $\text{Ga}_{15}$  geometries conform to symmetry  $D_{3h}$ , and these units are linked within the gallium networks through twelve Ga–Ga external bonds involving the hexagons. The  $\text{Ga}_{15}$  geometries and their relative stabilities have been analyzed in a previous paper.<sup>16</sup>

(39) Schwarz, U.; Bräuninger, S.; Burkhardt, U.; Syassen, K.; Hanfland, M. *Z. Kristallogr.* **2001**, *216*, 331–336.

(40) Yatsenko, S. P.; Semyannikov, A. A.; Semenov, B. G.; Chuntunov, K. A. *J. Less-Common Met.* **1979**, *64*, 185–199.

(41) Pearson, W. B. *J. Solid State Chem.* **1985**, *56*, 278–287.

(42) Nesper, R. *Angew. Chem., Int. Ed. Engl.* **1991**, *30*, 789–817.

(43) Bobev, S.; Bauer, E. D.; Thompson, J. D.; Sarrao, J. L. *J. Magn. Mater.* **2004**, *277*, 236–243.

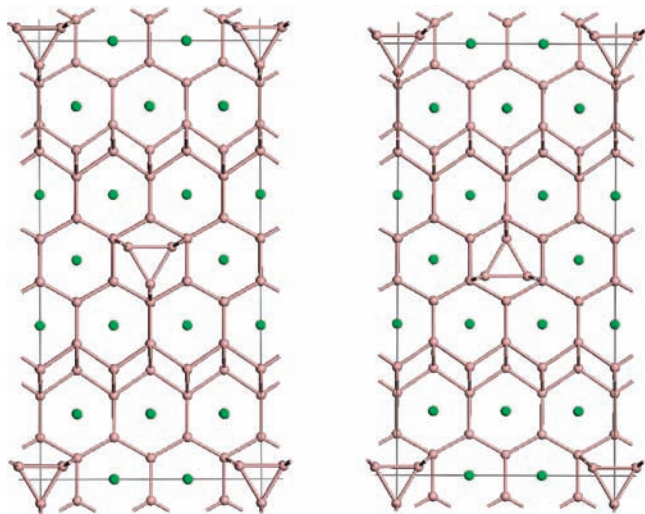


**Figure 7.**  $\text{Yb}_{16}\text{Ga}_{54}$  ordered models, *Immm2* (left) and *Pmm2* (right), built in a  $1 \times 3 \times 1$  supercell of dimensions  $a = 4.24$ ,  $b = 13.11$ ,  $c = 25.97$  Å. They only differ by the relative orientation (parallel or antiparallel) of triangles.

In  $\text{YbGa}_{3,34}$ , the severe randomized disorder most certainly accounts for the spurious appearance of space group *Immm*. Unfortunately, the absence of any extra reflections in the collected data set made impossible the resolution of the structure in a larger unit cell, so we just used this space group to approach the genuine structure. To gain better insight into the real atomic arrangement in  $\text{YbGa}_{3,34}$ , DFT geometry optimizations were performed by VASP using two likely ordered models built with respect to this stoichiometry. Both models, *Immm2* and *Pmm2*, represented by  $1 \times 3 \times 1$  supercells of dimensions  $a = 4.24$ ,  $b = 13.11$ ,  $c = 25.97$  Å contain 16 Yb and 54 Ga atoms. All atoms but gallium on triangles are reproduced from the original cell by appropriate translations along the  $b$ -axis. Triangles that substitute for Yb at  $0\ 0\ 0$  and  $1/2\ 1/2\ 1/2$  were given parallel orientations in *Immm2* and antiparallel orientations in *Pmm2* (Figure 7). The gallium independent atomic positions at triangles are  $0\ 0.098\ 0.030$  and  $0\ 0\ 0.949$  in the *Immm2* model and  $1/2\ 1/2\ 0.549$ ,  $1/2\ 0.597\ 0.462$ ,  $0\ 0.099\ 0.019$ , and  $0\ 0\ 0.935$  in the *Pmm2* model. VASP geometry optimizations, by varying atom positions and cell parameters, were done with respect to  $P1$  symmetry. Cell parameters did not deviate by more than 1.6% in *Immm2* and by more than 5.6% in *Pmm2*. VASP energies of formation clearly indicated the *Immm2* model to be the most stable ( $-1405.36$  kcal/mol against  $-1356.51$  per  $\text{Yb}_8\text{Ga}_{27}$  formula). The electronic structures of these  $\text{YbGa}_{3,34}$  models, with a substantial density of states at Fermi level, involving mainly the Yb 5d and Ga 4p states, are indicative of some metallic character (Figure 8). The  $\text{Ga}_{15}$  moieties do not behave as individualized closed shell units, as indicated by the good match between partial (projection on  $\text{Ga}_{15}$  atoms) and total density of states (DOS) in the whole energy domain. As already reported,<sup>44</sup> Mulliken charges are basis set dependent and then of limited use when calculated with CASTEP; they have to be taken on a relative scale. Gallium atoms in rhombic layers of  $\text{YbGa}_{3,34}$  bear charges that are similar to those in  $\text{YbGa}_4$ ,  $-0.28$  at 5-coordinated and close to zero at 4-coordinated atoms. Within the hexagon-based ribbons, the

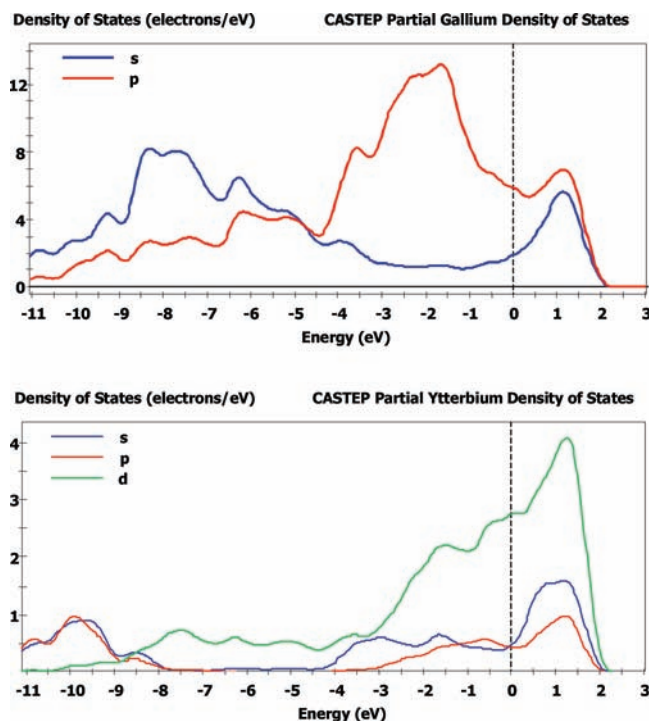


**Figure 8.** CASTEP partial densities of states for gallium and ytterbium in the *Immm2*  $\text{Yb}_{16}\text{Ga}_{54}$  model.

largest negative charges are also found for high coordinated atoms. A charge of  $-0.35$  is found for the hexagon atoms bonded to triangles, these atoms attract most of the negative density while the remaining atoms on hexagons and triangles bear lower charges varying from  $-0.05$  to  $-0.12$ .

In the best model *Immm2*, in which triangles are in parallel orientation, refined interatomic distances within the  $\text{Ga}_{15}$  unit are in the average of Ga–Ga distances encountered in gallium frameworks. The crystallographically underestimated triangle-to-hexagon distances of 2.327 and 2.357 Å refined to 2.482–2.502 Å, distances of 2.527 and 2.567 Å in the inner triangle changed to 2.562–2.574 Å while distances in the basal hexagons increased from 2.482–2.498 Å to 2.606–2.623 Å.

### Concluding Remarks

From a structural point of view, the gallium-rich domains in the lanthanide-gallium binary phase diagrams are very complex. Different studies have now provided some insights into the understanding of these systems. Both Sm–Ga and Yb–Ga diagrams contain an intermediate solid solution. In the case of Sm, the stoichiometry range is 13 at. % including compound  $\text{SmGa}_2$  at its Ga-poor border whereas for Yb, it is very narrow (2.4 at. %) and does not include the line compound  $\text{YbGa}_2$  which lies at 5 at. % beyond the Ga-poor limit. In a previous paper, we explained how enrichment in gallium yields structures that are reminiscent of the genuine graphite-like layers in  $\text{SmGa}_2$ .<sup>16</sup> This proceeds through the progressive and statistical replacement of Sm atoms by  $\text{Ga}_3$  triangular units (in  $\text{SmGa}_{2.67}$ ) up to a threshold located around  $\text{SmGa}_{3.64}$ , from which, as steric hindrance increases, only smaller gallium units (dumbbells) are allowed to substitute for Sm.

More compounds are found in the Ga-rich part of the Yb–Ga system; they also display complex and sometimes

(44) Lacroix-Orio, L.; Tillard, M.; Belin, C. *Solid State Sci.* **2008**, *10*, 5–11.

disordered structures.  $\text{YbGa}_2$ , with a diamond-like network of 4-coordinated gallium atoms, is structurally different from  $\text{SmGa}_2$  (graphite-like). With extremely close compositions,  $\text{YbGa}_{2.64}$  and  $\text{Yb}_3\text{Ga}_8$  ( $\text{YbGa}_{2.67}$ ) are however very different. The former, with hexagonal layering in which some Yb atoms are replaced by  $\text{Ga}_3$  units, is similar to  $\text{SmGa}_{2.67}$ .  $\text{Yb}_3\text{Ga}_8$  is orthorhombic ( $a \approx b$ ) and contains intergrown rhombic (4- and 5-coordinated Ga) and hexagonal (3-coordinated Ga) sublattices. In compound  $\text{YbGa}_{3.34}$ , which looks like  $\text{Yb}_3\text{Ga}_8$ , the increase in gallium leads to some substitution of  $\text{Ga}_3$  units for Yb atoms within the hexagonal sublattice. Building of

$\text{YbGa}_4$  from  $\text{YbGa}_{3.34}$  may be assimilated to a collapse of the structure after removal of the hexagonal sublattice enabling direct interlinking of rhombic layers (4- and 5-coordinated Ga). Surprisingly, for  $\text{YbGa}_5$ , a crossed hexagonal sublattice comes again in between rhombic layers. At last, the Ga-richer compound  $\text{YbGa}_6$  only contains a twisted crossed hexagonal lattice built of 3- and 5-coordinated Ga atoms.

**Supporting Information Available:** Crystallographic information files (CIF). This material is available free of charge via the Internet at <http://pubs.acs.org>.